



Enhanced Antimicrobial and Cytotoxicity on Cancer Cell using Bio-Originated Selenium Nanoparticles

A. DHIVYA¹, RAKHI YADAV^{1,*} and K. PANDIAN²

¹Department of Chemistry, Madras Christian College, University of Madras, East Tambaram, Chennai-600059, India

²Department of Inorganic chemistry, University of Madras, Guindy Campus, Chennai-600025, India

*Corresponding author: Email: rakhiyadavres@yahoo.co.in

Received: 27 August 2019;

Accepted: 19 October 2019;

Published online: 31 January 2020;

AJC-19755

Present work describes the bio-originated synthesis of selenium nanoparticles using seed extract of *Cassia angustifolia*. The biological macromolecules in seed extract react with metal ions to generate selenium nanoparticles. The seed extract acts as reducing, capping and stabilizing agents. The selenium nanoparticles produced by the plant extract are amorphous, nearly spherical in shape and held together by protein coating in a range of about 80-100 nm in size, under ambient conditions. The structural properties of selenium nanoparticles were characterized by UV-visible spectroscopy, FTIR, XRD, FESEM with EDAX, HRTEM and AFM. Antibacterial and antifungal activity of selenium nanoparticles were tested against four bacterial and two fungal strains using standard agar-well diffusion method. The zone of inhibition was observed in the selenium nanoparticles against different microbes and suggested that the bio-originated selenium nanoparticles act as an effective antibacterial and antifungal agent, so it has a great latent in the preparation of drugs used against pathogenic diseases. The cytotoxicity of bio-originated selenium nanoparticles was tested under *in vitro* conditions on Vero cell line and had compared with MDA-MB231 cancer cell line at different concentrations and the results had proved that bio-originated synthesis selenium nanoparticles can inhibit the growth of human breast-cancer cells by concentration-dependent manner.

Keywords: Biooriginated synthesis, Selenium nanoparticles, *Cassia angustifolia*, Antimicrobial activity, Cytotoxicity.

INTRODUCTION

Regarding scientific development, nanotechnology has increased critical ground in giving nano-estimate material for cancer treatment [1,2]. Biogenic synthesis of nanoparticles utilizing of bioorganic materials as bacteria, fungi and plants progressively moderate and increasingly securable since it uses eco-accommodating routes of synthesis from non-lethal materials [3]. Biogenic amalgamation of nanoparticles have been transmitted as an easy strategy for merger assortment of inorganic nanomaterial almost optimizing temperature, concentration, response time and pH [4].

Selenium a trail elementary component for human nourishment, is best known as a co-factor for some imperative proteins like glutathione peroxidase (GPx), thioredoxin reductase (TRx) and deiodinases. These proteins do imperative jobs against oxidation, generation and muscle work [5]. Se-protein blended by plants and creatures contain Se-Met; which is the central

type of selenium in oats and different plants [6]. Selenoproteins are normal in Brazil nuts and selenium amassing plants, similar to onion, garlic and mushrooms [7]. Yeast can be all around used for selenium dietary supplementation as they have great capacity to combine selenoproteins [8]. The biogenic nanoform of selenium from distinctive bacterial strains and plants exist that can lessen the lethal ionic type of selenium to non-harmful basic selenium. Lately, selenium has developed as a vital part in the dietary remedial action of numerous sorts of cancer growth [5]. Selenium nanoparticles (SeNPs) when contrasted with a few broadly considered selenium compounds like sodium selenite, seleno-methionine and methyl selenocysteine, were accounted for to display extraordinarily to bring down intense danger and sub-chronic toxicities. Also, it was identically viable in its capacity to increase selenoenzyme [9-11]. The most widely recognized selenium types of our biosphere are the inorganic selenium salt like selenite (Se⁴⁺), selenate (Se⁶⁺) and selenide (Se²⁻) [12]. A few examinations [9,11] have found that basic

selenium is considered as a least dangerous than selenium metal ions. The comparative impact of SeNPs and selenomethionine supplementation, SeNPs seemed to be more successful than that of natural selenomethionine in expanding muscle selenium content [13].

Nano-sized selenium generation has two different ways viz. chemical and organic courses [14]. Raised temperature and high pressure associated with the chemical synthesis of selenium nanoparticles are hazardous to the environment [15, 16]. The least complex strategy for balancing the particles by a single layer coating of polymer or surfactant, which is a thick lattice; this outcomes in an expansion of consistency and decreases the collaboration between the nanoparticles inhibiting agglomeration. The coating helps in securing the nanoparticle as well as it helps the conjugation of nanoparticle with biomacromolecules [17]. There are a few reports which articulate to balance the SeNPs by the utilization of a few covering specialists like polymers, surfactants or different biocompatible operators. The SeNPs using bovine serum albumin (BSA) shows an expanded size of particles of around 100 nm while these particles without the coating were of 40-60 nm [18].

The metabolites in plants like sugars, phenolic mixes, flavonoids, tannins, saponins, minerals, vitamins, potassium, calcium are known to be potential reducing agent of selenium [19] and it represent a better alternative to chemical methods to fulfil the developing interest for non-hazardous nanoparticle synthesis routes [20]. Nano-selenium employs through the plant extract which is more useful in the field of nanomedicine. There are a few reports in the literature with respect to the synthesis of selenium nanoparticles utilizing plants. They are leaves of lemon [21], *Terminalia arjuna* [22], raisin concentrate of grapes [12], *Capsicum annum* extract [23] and seed extract of fenugreek [24], β -lactoglobulin [25], arabic gum [26], ginger [27], garlic cloves [28] and polysaccharides like chitosan, konjac glucomannan, acacia gum, carboxymethyl cellulose [29]. The biologically incorporated SeNPs had diverse retention maxima than chemically integrated nanoparticles. The formation of nanoparticles by this technique is incredibly quick, requires no poisonous chemicals and the nanoparticles are steady for several months [30]. To produce precise size and shape of selenium nanoparticles, different variation like change in biological source, sodium selenite concentration, temperature, pH, aeration and reaction time. An endeavour was made to synthesize biocompatible selenium nanoparticles utilizing plants as reducing agent. For this reason, nearly 25 plants were screened, among them, *Cassia angustifolia* aqueous seed extract supported the synthesis of highly effective and stable SeNPs. The seed extract of *Cassia angustifolia* act as both reducing and stabilizing agent which gives selenium nanoparticles exhibit powerful chemo preventive and chemotherapeutic agent [31].

The present work discusses the reduction of selenite to SeNPs by using seed extract of *Cassia angustifolia*. *Cassia angustifolia* (family: Caesalpinaceae) is a quickly developing and spreading Indian shrub. The plant parts seeds, pods and leaves are broadly used for pharmaceutical applications. *Cassia angustifolia* seed contains biomolecules like galactomannan, galactopyranose, mannopyranose, triterpenoid glycoside-saponin [32] flavonoids like quercimeritin, scutellarein, rutin

[33], anthraquinone derivatives like rhein, alo-emodin, emodin, physcion, chrysofanol [34] and dianthrone derivatives sennoide A and B [35]. These biomolecules in *Cassia angustifolia* seed extract serves as bio-reducing, bio-stabilising and natural capping agent for nanoparticles.

Selenium nanoparticles (SeNPs) conjugated with ascorbic acid achieve enhanced antibacterial activity [36]. Inhibition of Gram-negative and Gram-positive bacteria by SeNPs with same efficacy [37]. Antifungal activity was reported in focussing SeNPs [38], usage of selenium nanoparticle as trace element in inhibition of *Aspergillus niger* [39]. SeNPs are able to inhibit the human breast-cancer cell (MCF-7) growth by dose-dependent manner [24]. Polysaccharide-mediated SeNPs that triggered cell death in A375 human melanoma cells [40]. Cytotoxicity of SeNPs toward several human cancer cell lines SPS-SeNPs with spirulina polysaccharides [41]. Mushroom polysaccharides-protein complexes inhibit the growth of MCF-7 human breast carcinoma cells [42]. Among the various sources of anticancer drugs, selenium nanoparticles have more advantages regarding to the potentials. In this study, the aim is to find a new source of low or non-toxic, antimicrobial and anticancer agent selenium nanoparticles, generated using *C. angustifolia* seed extract. Bio-originated selenium nanoparticle shows antimicrobial activity, cytotoxicity with Vero (normal) and MDA-MB-231 (cancer) cell lines.

EXPERIMENTAL

Cell culture Dulbecco's modified eagle medium (DMEM) and fetal bovine serum (FBS), 0.25 % trypsin-EDTA were purchased from Gibco (Grand Island, NY, USA). Streptomycin, penicillin, dimethyl sulfoxide, [3-(4,5-dimethylthiazol-2-yl)-2,5-diphenyltetrazolium bromide] (MTT), sodium selenite (Na_2SeO_3) and ethanol was purchased from Loba Chemicals, Pvt. Ltd, India. Double distilled water was used for the preparation of all stock solution

Preparation of plant extract: *Cassia angustifolia* seeds were collected from Tuticorin district, India. The plant seeds were brought to laboratory and washed with distilled water then dried. The seeds were grounded with motor pestle into fine powder and then sewed with micron size mesh. About 5 g of seed powder was taken in a conical flask and 50 mL of distilled water was added. Then, the reaction mixture was heated in a water bath for 80°C for the duration of 15 min until the colour of the solution changes to yellow. Then the mixture was cooled to the room temperature and filtered with Whatman No.1 filter paper to remove the solid materials. The collected filtrate was stored until further use.

Synthesis of selenium nanoparticles: Selenium nanoparticles were prepared according to the reported method [24]. Seed extract (2 mL) was mixed drop by drop in 20 mL of 0.01 M sodium selenite solution under magnetic stirring. The mixture was incubated in rotatory orbital shaker operating at 100 rpm at 30°C in a dark condition maintaining pH 5, at 24 h, the small amount of reaction medium was analyzed for absorbance from 200 to 700 nm using UV-vis HITACHI U-2900. After 72 h of incubation, the solution was centrifuged at 7000 rpm for 15 min. The red selenium nanoparticles were washed with double distilled water and ethanol and dried.

FTIR analysis: To identify the biomolecules, present in the seed extract of *Cassia angustifolia* and synthesized SeNPs samples were analyzed by FTIR spectroscopy (FTIR Hitachi 270-50, Japan). The synthesized SeNPs were lyophilized and used in the FTIR analysis, performed with KBr pellets in the range of 4000-400 cm^{-1} .

XRD analysis: The crystallographic structures of biogenic selenium nanoparticles phase properties were revealed by XRD measurements. Powder X-ray diffractometry (SEIFERT JSO-DEBYEFLEX 2002) was used to study the nature of SeNPs. The XRD pattern was scanned in the 2θ range from 30° to 70° with step size 0.04° per second.

FESEM with EDAX measurements: SEM samples of SeNPs were prepared by dispersing it on a copper flake and then evaporating gold onto them. FESEM measurements were carried out on a JEOL-JSM-6700F instrument operated at an accelerating voltage of 5 kV.

HRTEM analysis: TEM samples of SeNPs synthesized using *Cassia angustifolia* seed extract were prepared and placed on carbon coated copper grids. JEOL model 1200EX instrument used for TEM measurements operated at an accelerating voltage of 80 kV.

Atomic force microscopy (AFM) analysis: The AFM would give data about the 3D profile as well as the sponginess with the use of Model-Nano-Surf easy scan 2 AFM, Switzerland. A clean glass plates was cut into $1\text{ cm} \times 1\text{ cm}$ dimension, about 1 mg/mL concentration of SeNPs were prepared in ethanol, a drop of SeNPs suspension was placed on clean glass plates and kept in vacuum desiccator overnight, a thin film was formed over the glass plates. The dried nanoparticle suspension was scanned by AFM in a room temperature at the scan rate of 0.996 Hz. Atomic force microscopy used to analyze the particle size and distribution, porosity, surface roughness and morphology of SeNPs, while the 3D image gives information about the surface roughness.

Agar well diffusion method: The antimicrobial activities of biogenic selenium nanoparticles were carried out by agar well-diffusion method. Total six microbes namely, four different human pathogenic bacteria *E. coli* ATCC 8739, *P. aeruginosa* ATCC 27853 (Gram-negative), *B. subtilis* ATCC 6633, *S. aureus* ATCC 29736 (Gram-positive) and two fungi pathogens, *C. albicans* ATCC 2091, *A. niger* ATCC 1015 were selected for the present investigation.

The young microbial inoculums were prepared and the tube was incubated at 37°C until the turbidity was reached up to 0.5 McFarland standards [Twelfth Information Supplement, 2002 NCCLS (National Committee for Clinical Laboratory Standards), M100-S12 Performance Standards for Antimicrobial Testing]. The petri-plates were washed and placed in an autoclave for sterilization. After sterilization, nutrient agar medium and PDA medium were poured into each sterile petri plate and allowed to solidify in a laminar air flow chamber. After solidification, using a sterile cotton swabs, fresh microbial cultures were spread over the plate by spread plate technique. Wells of 5 mm size made into the agar plates with the help of sterile corkborer, the wells were loaded with 50 μL of seed extract, 50 μL of 10 mM synthesized selenium nanoparticles and gentamycin (1 mg/mL) was used as a positive control for

bacterial strains while fluconazole (1 mg/mL) was used in case of fungal pathogen. For 24 h, all the plates were incubated at 37°C . After incubation, the plates were observed for formation of clear inhibition zone around the well, indicates the presence of antimicrobial activity. Zone of inhibition was measured after incubation with Hi-Media scale by measuring the diameters of the inhibition zone [43]. The lowest concentration of the nanoparticles that inhibit the visual growth of tested organism as minimum inhibitory concentration (MIC). To determine MIC different concentrations of selenium nanoparticles (10, 20, 30, 40 μL) were added to different wells and zone was measured.

Cell culture maintenance: Vero African green monkey kidney normal cell line and MDA-MB-231 breast cancer cell line were obtained from the National Centre for Cell Sciences (NCCS), Pune, India. Cells were maintained in the logarithmic phase of growth in DMEM medium that supplemented with 10 % (v/v) heat inactivated fetal bovine serum, 100 $\mu\text{g}/\text{mL}$ penicillin, 100 $\mu\text{g}/\text{mL}$ streptomycin. They were maintained at 37°C with 5 % CO_2 - 95% air humidified incubator.

Effect of selenium nanoparticles on cytotoxicity of cell lines-MTT assay: The cytotoxic effect of SeNPs synthesized from the aqueous seed extract of *Cassia angustifolia* tested against both normal cell line and cancer cell line by MTT (3-(4,5-dimethylthiazol-2-yl)-2,5-diphenyltetrazolium bromide) assay [44,45]. Briefly, cell lines were separately seeded in 96-well microplates (1×10^6 cells/mL) and incubated at 37°C for 24 h with 5 % CO_2 incubator and allowed them to grow to 90 %. At the end of incubation, medium was replaced and the Vero cell were treated with SeNPs at different concentrations of 10, 20, 30,40 and 50 $\mu\text{g}/\text{mL}$. Subsequently, cancer cell line also treated with SeNPs at same concentrations. Then the samples were incubated for 24 h. The cells were then washed with phosphate buffered saline (PBS, pH-7.4) and added 20 μL of MTT solution (5 mg/mL) to each well and allowed to stand at 37°C in the dark for additional 4 h. Then, added 100 μL DMSO and dissolved the formazan crystals and its absorbance was read spectrophotometry at 570 nm using ELISA plate reader. The percentage of cell viability was expressed as:

$$\text{Cell viability (\%)} = \frac{\text{Absorbance of treated cells}}{\text{Absorbance of control cells}} \times 100$$

Anticancer studies: The concentration that inhibited 50 % of cell growth was referred as IC_{50} value, which was used as a parameter for cytotoxicity study. The morphological changes of untreated (control) and the cells treated at IC_{50} were observed under bright field microscope after 24 h.

RESULTS AND DISCUSSION

UV-visible analysis: The colourless solution of sodium selenite contains selenium ions turns pale-yellow seed extract into red colour selenium nanoparticles. Fig. 1a indicates the reduction of selenite ions to selenium nanoparticles by visual observation. Wavelength ranging from 200 to 700 nm is observed to mediate selenium nanoparticles. The red colloidal solution exhibited absorption maxima at 286 nm. Initial small peak absorbed in the UV region may be due to trace amount of organic molecule shown in Fig. 1b. This UV data support to further

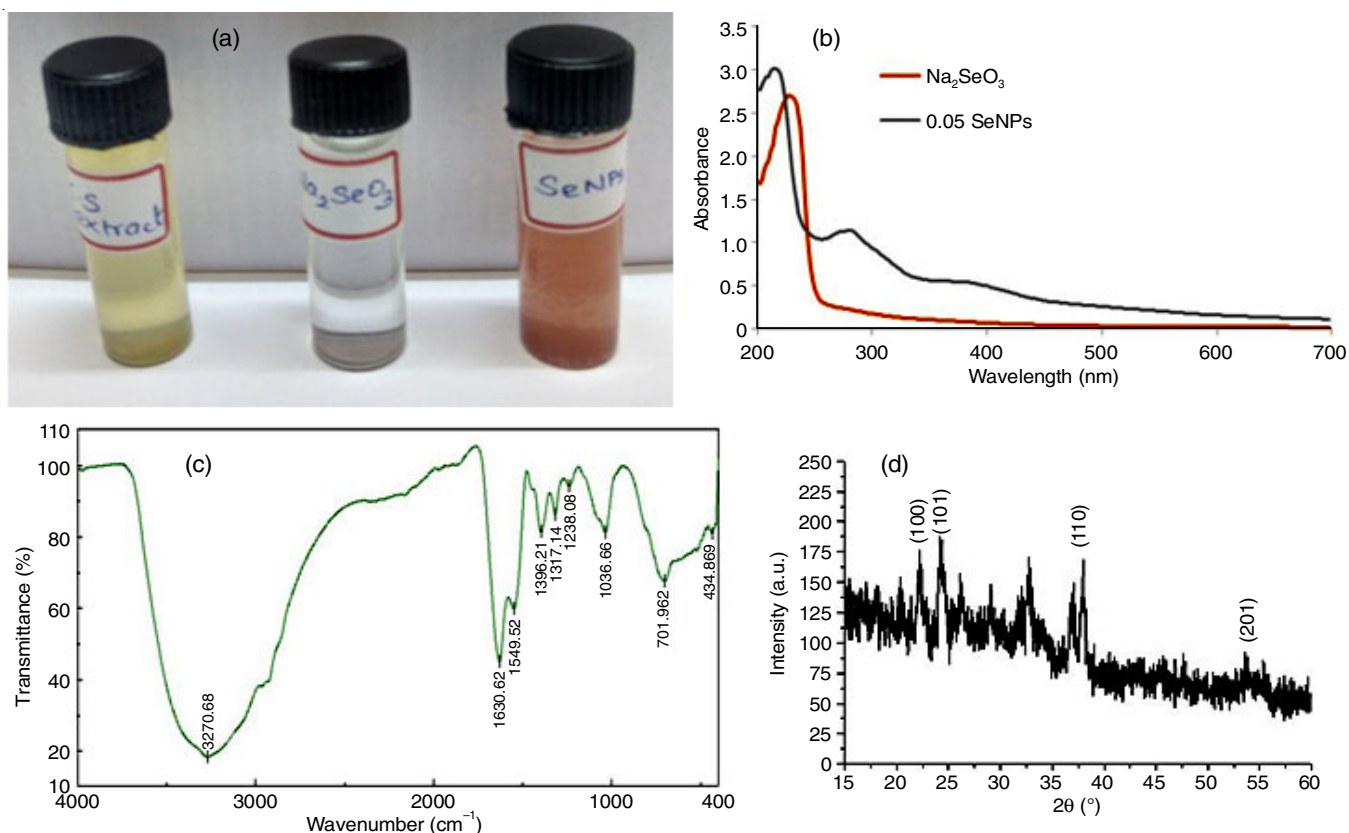


Fig. 1. (a) Colour change of reaction solution, (b) UV visible spectrum of sodium selenite and SeNPs, (c) FTIR of SeNPs, (d) XRD pattern of SeNPs

characterization of selenium nanoparticles. Fesharaki *et al.* [46] and Zare *et al.* [47] have observed absorption maximum (λ_{\max}) as 265 nm and at 245 nm, respectively.

FT-IR analysis: FT-IR spectral data for the bio-originated selenium nanoparticles is shown in Fig. 1c. The major absorption bands appeared at 3270.68, 1630.52, 1549.52, 1396.21, 1317.14, 1328.08, 1036.55, 701.962 and 434.896 cm^{-1} . The peak located at 3270.68 cm^{-1} shows O-H (of alcohol) and N-H group gets broad in the formation of selenium nanosphere [26]. A peak at 1630.52 cm^{-1} is assigned for C=O (of acid) and C=C stretching in aromatic ring. The peaks at 1396.21 and 1317.14 cm^{-1} attributed for C-N (of amines). The peak at 1036.55 cm^{-1} shows C-O stretching (of amino acids), while the peaks at 701.962 and 434.896 cm^{-1} shows C-H out of plane bending.

XRD analysis: The crystal structure and phase composition of SeNPs are determined using XRD technique. The peaks emerging at 22.41° (100), 24.32° (101), 37.95° (110), 53.86° (201), which are in a good agreement with literature value (JCPDS card no. 06-0362) [24]. In bio-originated synthesis, some noise background is seen due to the presence of some additional bioactive compound present in *Cassia angustifolia* seed extract. The broadening of peak shapes in the XRD pattern clearly indicates the particles are amorphous in nature as shown in Fig. 1d.

FESEM analysis with EDAX: The FE-SEM is used to visualize very small topographic structure of particle and the distinction of different phases. Usually selenium tends to form a spherical morphology with uniform diameter and smooth surface, and the surface is easily coated by other material due to reduction and disproportionation [36]. The size of selenium

nanoparticle indicates the range from 80 to 100 nm (Fig. 2a). The smaller size spherical selenium nanoparticle synthesized in this study will be highly beneficial for the drug delivery and thereby it will help for the field of biomedical applications. The EDAX confirms the elemental nanoparticle synthesized by seed extract of *Cassia angustifolia* as shown in Fig. 2b. The reported identical lines for the major emission energies for SeL α , SeK α and SeL β are 1.37, 11.22 and 12.49 keV, respectively [24]. The peaks in the spectra confirms that selenium has been suitably identified.

HRTEM analysis: HRTEM is used to characterize the size and morphology of the biogenic selenium nanoparticles. The spherical ball-like structure of selenium nanoparticles in the TEM images ranged in size from 80-100 nm in diameter. Fig. 2c shows selenium nanoparticles at 200 nm scale. A thin film encapsulating the nanoballs confirm the presence of a capping agent covering and stabilizing the nanoballs.

Atomic force microscopy (AFM) analysis: Fig. 2e shows the AFM spectral image of selenium nanoparticles synthesized using *Cassia angustifolia* seed extract with a scanning area of 2.461 μm^2 between 0 m X 6.19 μm and 0 m Y 6.19 μm . Spherical shaped selenium nanoparticles [27] were found with size in the range 80-100 nm. The size and shape can be measured from topographic and cross section analysis. The results are comparable with the FESEM and HRTEM results.

Antimicrobial activity of selenium nanoparticles (SeNPs): To perform the antimicrobial activity of SeNPs, well diffusion method was adopted for experimental microbes show a clear zone of inhibition which was compared with control.

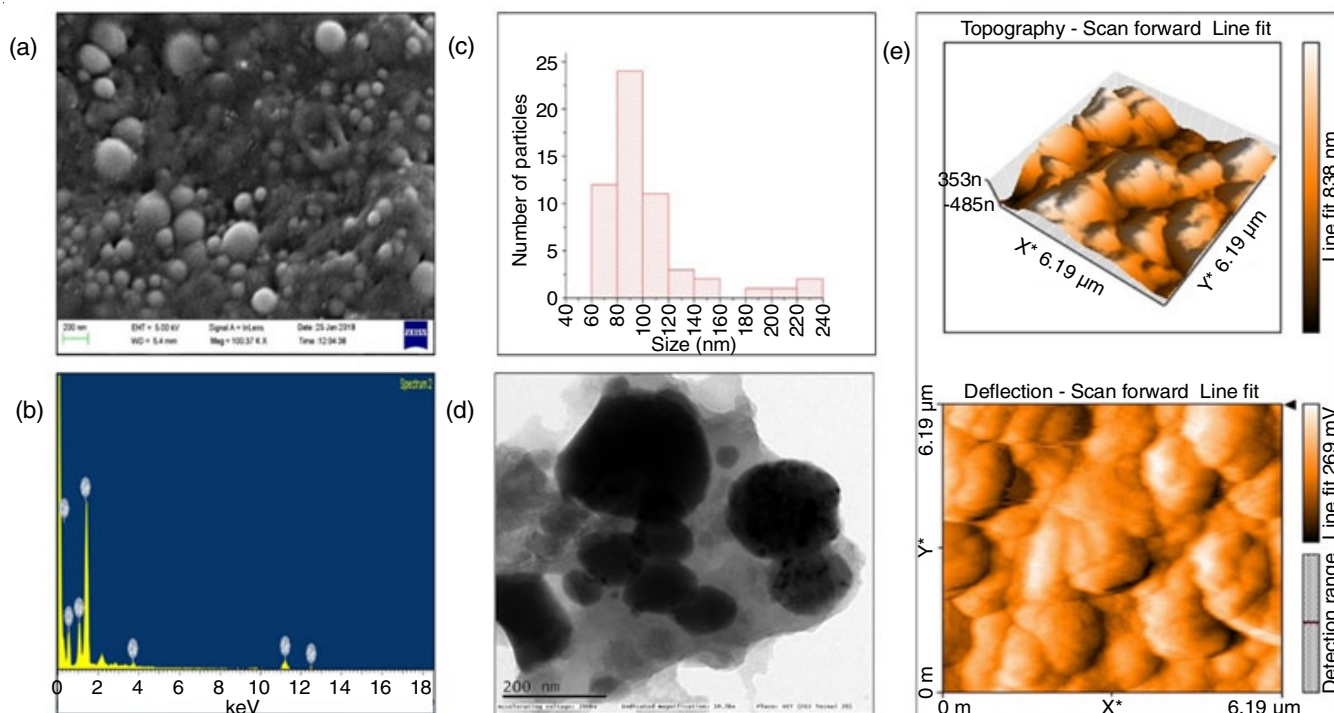


Fig. 2. (a) FESEM of SeNPs, (b) EDAX of SeNPs, (c) Histogram of SeNPs, (d) HRTEM of SeNPs, (e) AFM images of SeNPs

The zone of inhibition of *Cassia angustifolia* seed extract was not seen. The antibacterial activity of SeNPs was effective against *S. aureus* (18 mm), *B. subtilis* (16 mm), *E. coli* (17 mm) and *P. aeruginosa* (15 mm). The antifungal activity showed a maximum susceptibility to the administration of selenium nanoparticles with an inhibition zone of *Candida albicans* (11 mm) and *Aspergillus niger* (20 mm), respectively. The minimum inhibitory concentration was checked with the same experimental pathogenic bacteria and fungi at different dosage of SeNPs such as 10, 20, 30, 40 μL . When the concentration of 10 $\mu\text{g}/\text{mL}$ of SeNPs was used, only a slight zone of inhibition was seen. The zone of inhibition of tested microbes, control and minimum inhibitory concentration is shown in Table-1. The synthesized selenium nanoparticles were very effective in controlling the bacterial and fungal human pathogens. These results are compared with reported results [36,38].

Cell viability of bio-originated SeNPs against Vero (normal) and MDA-MB 231 (cancer) cell lines: SeNPs act as wonderful nanocarriers of anticancer drugs due to their cytocompatibility, stability and ease of binding with biomolecules in nanomedicine [48]. The cytotoxicity of SeNPs under *in vitro* conditions on Vero cells and MDA-MB 231 cells were tested

on cell proliferation by MTT assay. The effect of bio-originated SeNPs at different concentrations such as 10, 20, 30, 40 and 50 $\mu\text{g}/\text{mL}$ nanoparticles on cell viability of Vero cells and MDA-MB 231 cells was made at 24 h (Table-2). Verma *et al.* [49] reported that Vero cell lines at higher concentrations showed substantial cell mortality. SeNPs showed a maximum IC_{50} value of 10 $\mu\text{g}/\text{mL}$ followed by 50 $\mu\text{g}/\text{mL}$. SeNPs tested Vero cells showed better biocompatibility and significantly decreases the cell viability in treated concentrations when compared to control. The bio-compatibility of SeNPs was gradually increased at all concentrations by time. Here, it is believed that SeNPs are not chronically toxic to the cell growth. The Vero cells treated for 24 h with the respective IC_{50} concentration of SeNPs revealed that the cells became rounded, shrink and lose their contact with neighbouring cells (Fig. 3a). There was a significant decrease in the cell viability was recorded in treated concentrations when compared to control ($p < 0.05$) for cancer cell line. These results prove that SeNPs on increasing concentrations increase in the toxicity of cancer cell line. Fig. 3b was found irregular confluent aggregates, rounded and polygonal. As SeNPs concentration increases the treated cell shrunk and changed the shape and number of adhering cells decreased. The results are compared

TABLE-1
ZONE OF INHIBITION OF TESTED MICROBES

Tested microbes	Zone of inhibition (diameter in mm)					
	Control	Concentration of SeNPs (50 mM)	Minimum inhibitory concentration (MIC)			
			10 μL	20 μL	30 μL	40 μL
<i>Staphylococcus aureus</i>	20	18	5	9	11	13
<i>Bacillus subtilis</i>	27	16	3	7	10	11
<i>Pseudomonas aeruginosa</i>	21	15	4	6	8	12
<i>Escherichia coli</i>	19	17	6	10	12	13
<i>Candida albicans</i>	16	11	2	5	9	9
<i>Aspergillus niger</i>	–	20	7	13	15	17

Control* - Gentamycin (1 mg/mL) Positive control for bacterial strains; Fluconazole (1 mg/mL) Positive control for fungal strains.

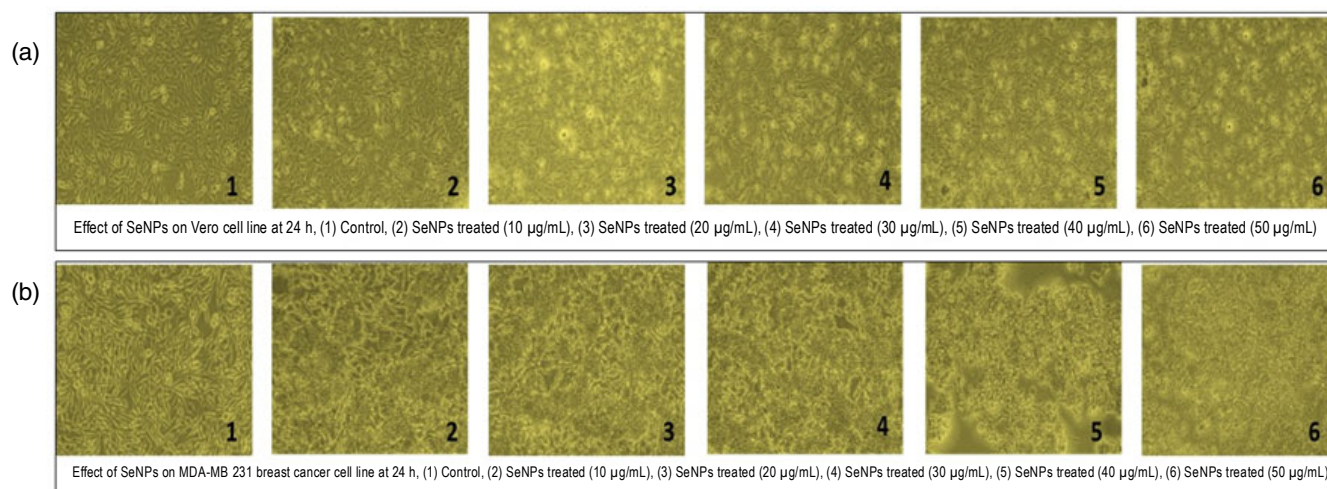


Fig. 3. (a) Microscopic image of Vero cells, (b) Microscopic image of MDA-MB-231 breast cancer cells

TABLE-2
PERCENTAGE INHIBITION OF VERO CELLS & MDA-MB-231 BREAST CANCER CELLS USING DIFFERENT CONCENTRATION OF SeNPs

	VERO cell line					MDA-MB 231 breast cancer cell line				
	I	II	III	Average	Inhibition (%)	I	II	III	Average	Inhibition (%)
Control	–	–	–	0.815000	100.000000	–	–	–	0.839000	100.000000
10 µg	0.775000	0.764000	0.771000	0.770000	94.478528	0.756000	0.763000	0.767000	0.762000	90.822408
20 µg	0.689000	0.695000	0.703000	0.695667	85.357873	0.667000	0.662000	0.676000	0.668333	79.658323
30 µg	0.629000	0.634000	0.623000	0.628667	77.137014	0.546000	0.552000	0.558000	0.552000	65.792610
40 µg	0.574000	0.584000	0.579000	0.579000	71.042945	0.415000	0.426000	0.420000	0.420333	50.099325
50 µg	0.493000	0.489000	0.498000	0.493333	60.531697	0.288000	0.304000	0.295000	0.295667	35.240366

*Control - Untreated cell line

with inhibition of cancer cell lines using gold nanoparticle [50]. Survival rate of normal cell was higher compared to cancer cell line at every concentration is shown in Table-2 (Fig. 4). Biological effect of SeNPs shows proliferation activity at different concentration is verified using a Vero and tumour cell lines of human breast carcinoma (MDA-MB-231). The bio-originated SeNPs were found to be potent, as evident by concentration (40 µg/mL) at which 50 % of cancer cell death occurred. Survival rate of MDA-MB-231 decreased to 35.24 % with 50 µg/mL of SeNPs.

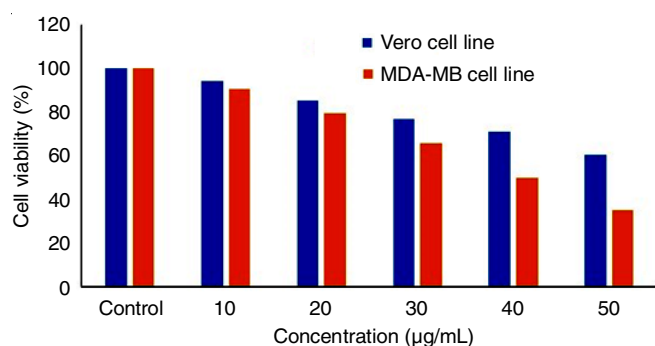


Fig. 4. Percentage of cell viability

Conclusion

The bio-originated selenium nanoparticles using *Cassia angustifolia* seed extract as green approach is investigated. Spectral techniques give a clear idea about the formation of

selenium nanoparticles. Spherical shape of selenium nanoparticles of 80-100 nm was confirmed from various tools in FESEM, HRTEM and AFM analysis. It is shown that selenium inhibits antibacterial and antifungal activities. In addition, the anti-cancer activity of selenium nanoparticles is found to be potent as the synthesized SeNPs were found to be toxic for the cancer cell than the normal cell line.

CONFLICT OF INTEREST

The authors declare that there is no conflict of interests regarding the publication of this article.

REFERENCES

- X. Shi, S.H. Wang, M. Shen, M.E. Antwerp, X. Chen, C. Li, E.J. Petersen, Q. Huang, W.J. Weber and J.R. Baker, *Biomacromolecules*, **10**, 1744 (2009); <https://doi.org/10.1021/bm9001624>
- S. Nie, Y. Xing, G.J. Kim and J.W. Simons, *Annu. Rev. Biomed. Eng.*, **9**, 257 (2007); <https://doi.org/10.1146/annurev.bioeng.9.060906.152025>
- S. Prabha, M. Dubey and L.M. Sillanpää, *Process Biochem.*, **45**, 1065 (2010); <https://doi.org/10.1016/j.procbio.2010.03.024>
- K.P. Kumar, W. Paul and C.P. Sharma, *Process Biochem.*, **46**, 2007 (2011); <https://doi.org/10.1016/j.procbio.2011.07.011>
- Y. Mehdi, J.L. Hornick, L. Istasse and I. Dufresne, *Molecules*, **18**, 3292 (2013); <https://doi.org/10.3390/molecules18033292>
- N.I. Barclay, *J. Food Compos. Anal.*, **8**, 307 (1995); <https://doi.org/10.1006/jfca.1995.1025>

7. E. Dumont, F. Vanhaecke and R. Cornelis, *Anal. Bioanal. Chem.*, **385**, 1304 (2006);
<https://doi.org/10.1007/s00216-006-0529-8>
8. A. Demirci, A.L. Pometto and J.D. Cox, *J. Agric. Food Chem.*, **47**, 2496 (1999);
<https://doi.org/10.1021/jf9811976+>
9. J. Zhang, X. Wang and T.T. Xu, *Toxicol Sci.*, **101**, 22 (2008);
<https://doi.org/10.1093/toxsci/kfm221>
10. J.S. Zhang, X.Y. Gao, L.D. Zhang and Y.P. Bao, *BioFactors*, **15**, 27 (2001);
<https://doi.org/10.1002/biof.5520150103>
11. H. Wang, J. Zhang and H. Yu, *Free Radic Biol Med.*, **42**, 1524 (2007);
<https://doi.org/10.1016/j.freeradbiomed.2007.02.013>
12. G. Sharma, A.R. Sharma, R. Bhavesh, J. Park, B. Ganbold, J.S. Nam and S.S. Lee, *Molecules*, **19**, 2761 (2014);
<https://doi.org/10.3390/molecules19032761>
13. X. Zhou, Y. Wang, Q. Gu, W. Li, X. Zhou, Y. Wang, Q. Gu and W. Li, *Aquaculture*, **291**, 78 (2009);
<https://doi.org/10.1016/j.aquaculture.2009.03.007>
14. S. Dhanjal and S.S. Cameotra, *Microb. Cell Fact.*, **9**, 52 (2010);
<https://doi.org/10.1186/1475-2859-9-52>.
15. W. Zhang, Z. Chen, H. Liu, L. Zhang, P. Gao and D. Li, *Colloids Surf. B Biointerfaces*, **88**, 196 (2011);
<https://doi.org/10.1016/j.colsurfb.2011.06.031>
16. S.K. Torres, V.S. Campos, C.G. Leon, S.M. Rodriguez-Llamazares, S.M. Rojas, M. Gonzalez, C. Smith and M.A. Mondaca, *J. Nanopart. Res.*, **14**, 1236 (2012);
<https://doi.org/10.1007/s11051-012-1236-3>
17. H. Lu, E.L. Salabas and F. Schüth, *Angew. Chem. Int. Ed.*, **46**, 1222 (2007);
<https://doi.org/10.1002/anie.200602866>.
18. P.A. Tran and T.J. Webster, *Int. J. Nanomed.*, **6**, 1553 (2011);
<https://doi.org/10.2147/IJN.S21729>
19. S. Barnaby, N. Sarker, A. Dowdell and I. Banerjee, *The Fordham Undergrad. Res. J.*, **1**, 41 (2011).
20. A.R. Ingole, S.R. Thakare, N.T. Khatri, A.V. Wankhade and D.K. Burghate, *Chalcogenide Lett.*, **7**, 485 (2010).
21. K.S. Prasad, H. Patel, T. Patel, K. Patel and K. Selvaraj, *Colloids Surf. B Biointerfaces*, **103**, 261 (2013);
<https://doi.org/10.1016/j.colsurfb.2012.10.029>
22. K.S. Prasad and K. Selvaraj, *Biol. Trace Elem. Res.*, **157**, 275 (2014);
<https://doi.org/10.1007/s12011-014-9891-0>
23. S. Li, Y. Shen, A. Xie, X. Yu, X. Zhang, L. Yang and C. Li, *Nanotechnology*, **18**, 405101 (2007);
<https://doi.org/10.1088/0957-4484/18/40/405101>
24. Ch. Ramamurthy, K.S. Sampath, P. Arunkumar, M.S. Kumar, V. Sujatha, K. Premkumar and C. Thirunavukkarasu, *Bioprocess Biosyst. Eng.*, **36**, 1131 (2013);
<https://doi.org/10.1007/s00449-012-0867-1>
25. J. Zhang, Z. Teng, Y. Yuan and Q.-Z. Zeng, *Int. J. Biol. Macromol.*, **107**, 1406 (2018);
<https://doi.org/10.1016/j.ijbiomac.2017.09.1172017>
26. H. Kong, J. Yang, Y. Zhang, Y. Fang, K. Nishinari and G.O. Phillips, *Int. J. Biol. Macromol.*, **65**, 155 (2014);
<https://doi.org/10.1016/j.ijbiomac.2014.01.011>
27. S. Menon, S. Devi K.S., H. Agarwal and V.K. Shanmugam, *Colloid Interf. Sci. Commun.*, **29**, 1 (2019);
<https://doi.org/10.1016/j.colcom.2018.12.004>
28. P.B. Ezhuthupurakkal, P.L. Rao, A. Suyavaran, A. Subastri and V. Sujatha, *Mater. Sci. Eng. C*, **74**, 597 (2017);
<https://doi.org/10.1016/j.msec.2017.02.003>
29. S.-Y. Zhang, J. Zhang and H.-Y. Wang, *Mater. Lett.*, **58**, 2590 (2004);
<https://doi.org/10.1016/j.matlet.2004.03.031>
30. R.S. Oremland, M.J. Herbel, J.S. Blum, S. Langley, T.J. Beveridge, P.M. Ajayan, T. Sutto, A.V. Ellis and S. Curran, *Appl. Environ. Microbiol.*, **70**, 52 (2004);
<https://doi.org/10.1128/AEM.70.1.52-60.2004>
31. A. Sweetey, *Appl. Microbiol. Biotechnol.*, **100**, 2555 (2016);
<https://doi.org/10.1007/s00253-016-7300-7>
32. R. Ahmed, K. Nagori, T. Kumar, M. Singh and D. Dewangan, *Int. J. Res. Ayurveda Pharm.*, **2**, 1320 (2011).
33. S.I. Ahmed, M.Q. Hayat, M. Tahir, Q. Mansoor, M. Ismail, K. Keck and B. Robert, *BMC Complement. Altern. Med.*, **16**, 460 (2016);
<https://doi.org/10.1186/s12906-016-1443-z>
34. H. Dave and L. Ledwani, *Indian J. Nat. Prod. Res.*, **3**, 291 (2012).
35. M. Srivastava, S. Srivastava, S. Khatoun, A.K.S. Rawat, S. Mehrotra and P. Pushpangadan, *Pharm. Biol.*, **44**, 202 (2008);
<https://doi.org/10.1080/1388200600686442>
36. A. Ananth, V. Keerthika and M.R. Rajan, *Curr. Sci.*, **116**, 285 (2019);
<https://doi.org/10.18520/cs/v116/i2/285-290>
37. H. Hariharan, N. Al-harbi, P. Karuppiah and S. Rajaram, *Chalcogenide Lett.*, **9**, 509 (2012).
38. A. Shahverdi, A. Fakhimi, G. Masavat, P. Fesharaki, S. Rezaie and S. Rezaayat, *World Appl. Sci. J.*, **10**, 918 (2010).
39. Z. Kazampour, M. Hossein, F. Yazdi and A. Shahverdi, *Iran. J. Microbiol.*, **5**, 81 (2013).
40. T. Chen, Y.S. Wong, W. Zheng, Y. Bai and L. Huang, *Colloids Surf. B Biointerfaces*, **67**, 26 (2008);
<https://doi.org/10.1016/j.colsurfb.2008.07.010>
41. F. Yang, Q. Tang, X. Zhong, Y. Bai, T. Chen, Y. Zhang, Y. Li and W. Zheng, *Int. J. Nanomed.*, **7**, 835 (2012);
<https://doi.org/10.2147/IJN.S28278>
42. H. Wu, X. Li, W. Liu, T. Chen, Y. Li, W. Zheng, C.W.Y. Man, M.K. Wong and K.H. Wong, *J. Mater. Chem.*, **22**, 9602 (2012);
<https://doi.org/10.1039/C2JM16828F>
43. C. Jayaseelan, A.A. Rahuman, S. Marimuthu, T. Santhoshkumar, A.V. Kirthi, A. Bagavan, K. Gaurav, L. Karthik and K.V. Rao, *Spectrochim. Acta A Mol. Biomol. Spectrosc.*, **90**, 78 (2012);
<https://doi.org/10.1016/j.saa.2012.01.006>
44. B. Yu, Y. Zhang, W. Zheng, C. Fan and T. Chen, *Inorg. Chem.*, **51**, 8956 (2012);
<https://doi.org/10.1021/ic301050v>
45. T. Mossmann, *J. Immunol. Methods*, **65**, 55 (1983).
46. P.J. Fesharaki, P. Nazari, M. Shakibaie, S. Rezaie, M. Banoee, M. Abdollahi and A.R. Shahverdi, *Braz. J. Microbiol.*, **41**, 461 (2010);
<https://doi.org/10.1590/S1517-83822010000200028>
47. B. Zare, S. Babaie, N. Setayesh and A.R. Shahverdi, *Nanomed. J.*, **1**, 13 (2013);
<https://doi.org/10.7508/NMJ.2013.01.002>
48. W. Jiang, B.Y. Kim, J.T. Rutka and W.C. Chan, *Nat. Nanotechnol.*, **3**, 145 (2008);
<https://doi.org/10.1038/nnano.2008.30>
49. S. Verma, S. Abirami and S. Mahalakshmi, *J. Microbiol. Biotechnol. Res.*, **3**, 54 (2013).
50. A. Parveen and S. Rao, *J. Cluster Sci.*, **26**, 775 (2015);
<https://doi.org/10.1007/s10876-014-0744-y>